

Structural properties of α -quartz under high pressure and amorphization effects

A. Di Pomponio and A. Continenza

Dipartimento di Fisica, Università degli Studi de L'Aquila, Coppito (L'Aquila), I-67010 L'Aquila, Italy

(Received 20 April 1993)

The behavior of crystalline α -quartz under hydrostatic pressure is studied via total-energy calculations based on the full-potential linearized augmented-plane-wave method, within the local-density approximation. By examining recent experimental data and our theoretical results, the structural properties of α -quartz near and above the transition to the amorphous state are determined. Our results indicate that the SiO_4 tetrahedra distort, with a regular and slight decrease of the mean distance Si-O; the interpolyhedral Si-O-Si angles and the O-O distances decrease below the smallest value experimentally observed on ordered silicates, with a dramatic reduction of the structural voids. The oxygen lattice tends towards an ideal close-packed configuration, perhaps highly instable.

I. INTRODUCTION

Silica is one of the most useful materials in modern technology, which finds a multitude of applications in electronic devices and in glass manufactures. SiO_2 layers deposited on Si are the basis of the MOSFET (metal-oxide-semiconductor field-effect transistors) that constitutes the core of very-large-scale integrated circuits. The excellent insulating properties of silicon dioxide and the comparatively simple and cheap growth techniques developed explain its predominant role in today's technology.

Silica is also important in geology, as it is one of the main constituents of the Earth's mantle.

Silicon dioxide occurs in a wide variety of forms,¹ each with its own range of thermodynamic stability. In most common SiO_2 polymorphs, the silicon atom is coordinated by four oxygen atoms in a tetrahedral configuration. Each oxygen atom is bounded by two silicon atoms and interconnects two SiO_4 units. At the equilibrium phase, the O-Si-O angles are very close to the ideal tetrahedral angle of 109.5° . The structural differences among these polytypes depend on the value of the Si-O-Si bond angle, while their symmetry properties strictly depend on the geometry in which the tetrahedra are linked together to form chains.

The enormous technological and fundamental importance of SiO_2 is the reason why its properties have been the object of many experimental and theoretical works. Nevertheless, up to now, first-principles calculations related to silica have been mainly performed on model clusters^{2,3} (orthosilicic and disilicic molecules) to improve the understanding of the properties of the Si-O bond, since a theoretical description of the full crystal structure is rather complex. These studies have given the opportunity to generate interatomic potentials (especially the Born-Mayer two-body potential) that have been used in classical molecular-dynamics simulations of SiO_2 structural phase transitions³⁻⁵ and of the silica amorphous phase.⁶

Actually, the mixed ionic and covalent nature of the Si-O bond and the complicated structure make this system

quite difficult to treat quantum mechanically. Up to two years ago, in fact, there were few *ab initio* solid-state calculations of the structural and electronic properties,^{7,8} almost all restricted to the equilibrium structure with the exception of one all-electron investigation of the new ultrahigh-pressure phase of silica,⁹ more stable than stishovite. More recently, some thorough *ab initio* studies of the equilibrium structure together with the analysis of pressure effects¹⁰ have appeared.

The investigation of the behavior under high pressure is, in fact, of great interest, since it is possible to get insights into the nature of the interatomic bonds and into the mechanical and electronic properties in limit conditions. This interest has been increased by recent experimental works^{11,12} which showed evidence of a order-disorder transition of some polymorphs of silica under pressure.

This direct crystalline-to-amorphous transition, observed in a number of oxides,^{13,14} is very important in light of the production of bulk amorphous materials with peculiar mechanical properties for technological applications.

The stable form of silica, α -quartz, exists at room temperature and for pressures below 3 GPa. At higher pressures α -quartz persists as a metastable structure, which gradually undergoes a phase transition to an amorphous state (the transition pressure is around 30 GPa), as experimentally observed by x-ray diffraction measurements on powdered samples.¹¹ Some other experimental results¹² suggest that the onset of this transition may occur even at lower pressures (approximately 15 GPa).

In this paper, we present an all-electron investigation on pressure effects on the structural properties of α -quartz near and above the amorphous transition. Using first-principles calculations we analyze phases at pressures far above this transition, which are impossible to reach experimentally, in order to understand the physical mechanisms which drive the transformation.

According to Hazen *et al.*¹² this transition is correlated to strains which tend to modify the Si-O-Si angles. On the other hand, theoretical analysis^{4,10,15} have indicated

that structural instabilities could occur when the oxygen atoms approach a cubic close-packed configuration, and the silicon becomes sixfold coordinated. A very recent investigation seems to identify into lattice shear instability the driving force responsible for quartz amorphization.¹⁰

From our investigation we find that the main effects induced by compression are represented by a slight distortion of SiO_4 tetrahedra and a rapid decrease of the interpolyhedral Si-O-Si angles and O-O distances below the smallest value experimentally observed in ordered silicates. These results are in good agreement with previous theoretical analysis¹⁰ and experiment,^{12,16} in the range of pressures reached to date. On the other hand, some features, such as Si-O distance and axial ratio c/a , differ quite substantially from the theoretical trends obtained by Chelikowsky *et al.*¹⁰ from pseudopotential calculations. We find that the mean distance Si-O is conserved, with a regular and very small decrease; at higher pressures it tends to a saturation value, which is not too far from the equilibrium value. As a difference with previous theoretical calculations, the behavior of the ratio c/a as a function of pressure reproduces well the experiment and, at maximum compression considered, its value matches very closely the corresponding value of the ideal body-centered-cubic array of the oxygen anions.¹⁵

II. COMPUTATIONAL DETAILS

A. Method

The unit cell of α -quartz contains nine atoms (three Si and six O) and its symmetry group allows for several free positional parameters. Therefore, in order to determine theoretically the equilibrium structure at each different pressure, a minimization of the total energy of the system as a function of all the free parameters is required. In addition, due to the complex nature of the electronic interactions, a first-principles description of this material is a very heavy computational task.

We used the local-density approximation (LDA) within density functional theory, as parametrized by Hedin and Lundqvist¹⁷ and the full-potential linearized augmented plane wave (FLAPW) method.¹⁸ Almost all materials are reliably treated within this “all-electron” method, which

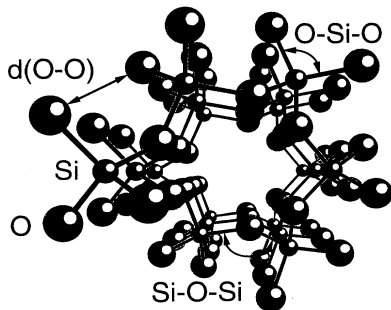


FIG. 1. Spiral of SiO_4 tetrahedra in α -quartz along the crystallographic c axis. The O-Si-O and the Si-O-Si bond angles and the interpolyhedral O-O distance are indicated.

TABLE I. Experimental unit cell constants (a , c in Å) and fractional coordinates from Ref. 16. The origin of the coordinate system is at $2/3c$ with respect to the choice of the *International Tables for X-ray Crystallography* (Ref. 23).

a	4.916 ± 0.001
c	5.4054 ± 0.0004
$x(\text{Si})$	0.4697 ± 0.0001
$x(\text{O})$	0.4135 ± 0.0003
$y(\text{O})$	0.2669 ± 0.0002
$z(\text{O})$	0.1191 ± 0.0002

allows to take into account the core states and does not make any assumption on the shape of the potential or the charge density, therefore overcoming the difficulties of pseudopotential methods with representing some chemical elements (for instance oxygen atoms).

We used a cut-off $R_{\text{max}} \cdot K_{\text{max}} = 6$ which, at the equilibrium experimental structure, results in about 830 basis functions. The technique of special \mathbf{k} points¹⁹ has been used for the \mathbf{K} -space integration (we considered three special \mathbf{k} points). The $2s$ and $2p$ states of O as well as the $3s$ and $3p$ states of Si were treated as valence states.

B. Structural details

The structure of α -quartz has trigonal symmetry, it belongs to the enantiomorphous crystal class 32, and its space group is D_3^6 ($P3_221$) or D_3^4 ($P3_121$) according to its right or left handedness.

In Fig. 1 we show a fragment of a spiral of SiO_4 tetrahedra in α -quartz along the crystallographic c axis. The O-Si-O and the Si-O-Si bond angles and the interpolyhedral O-O distance are shown.

The structure of α -quartz at room pressure has been refined by the x-ray diffraction method.²⁰ Moreover, the determination of the high-pressure structures has been performed via diffraction techniques, using both neutrons²¹ and x-rays.^{12,16,22}

The crystallographic data of Levien *et al.*¹⁶ at ambient pressure (D_3^6 space group) were used as reference in the present work (Table I). We point out that, following Levien *et al.*, we shifted of $2/3c$ the origin of the coordinates system along the threefold screw axis with respect to the choice of the *International Tables for X-ray Crystallography*.²³

III. RESULTS AND DISCUSSION

A. Geometry optimization and elasticity parameters determination

The pressure study has been performed as follows: For each fixed unit cell volume we optimized the structure (preserving the space group symmetry) by means of total-energy minimization with respect to the free configurational parameters.

There are three formula units per cell, but only two atoms are independent for symmetry: one silicon and one

oxygen at the 3(a) and 6(c) Wyckoff positions,¹ respectively. The structure is defined by six parameters: the lattice constants (a , c) and four fractional coordinates [$x(\text{Si})$, $x(\text{O})$, $y(\text{O})$, $z(\text{O})$]. Fixing the unit cell volume V , the total energy E becomes a function of five parameters. Since $V = \sqrt{3}/2a^2c$ (for an hexagonal cell), the natural choice is represented by the internal coordinates $x(\text{Si})$, $x(\text{O})$, $y(\text{O})$, $z(\text{O})$, and the c/a ratio.

We examined nine volumes and optimized the structure, via total-energy minimization, in each case. In Fig. 2(a) we report the calculated cohesive energy as a function of the volume. We fitted the E - V points using a Birch-Murnaghan²⁴ equation of state and determined the equilibrium cohesive energy E_0 , the volume V_0 , the zero-pressure bulk modulus B_0 , and its derivative with respect to the pressure, B'_0 .

In Table II we list a set of elasticity experimental data^{12,16,21,25} together with our and other theoretical results,¹⁰ for comparison.

The agreement between our theoretical values and experiment is fairly good. The Birch-Murnaghan equation of state fits excellently all experimental and theoretical points, as shown in Fig. 2(b).

The cohesive energy represents the energy per formula unit of the crystal with respect to the constituent atoms; the resulting binding energy is 24.57 eV/formula unit. In Table II this value is compared to experimental results²⁶ and other theoretical calculations.¹⁰ The overestimate of the theoretical cohesive energies is a typical finding of the local-density approximation.

The equilibrium volume agrees excellently with experiment (within $\sim 0.2\%$) and the bulk modulus too (within $\sim 1\%$ with respect to the value by Levien *et al.*¹⁶).

We note, in addition, that also the Murnaghan equation of state fits excellently the theoretical points and gives very similar results for the parameters (equilibrium volume and bulk modulus are within 0.2% and 4% deviation, respectively).

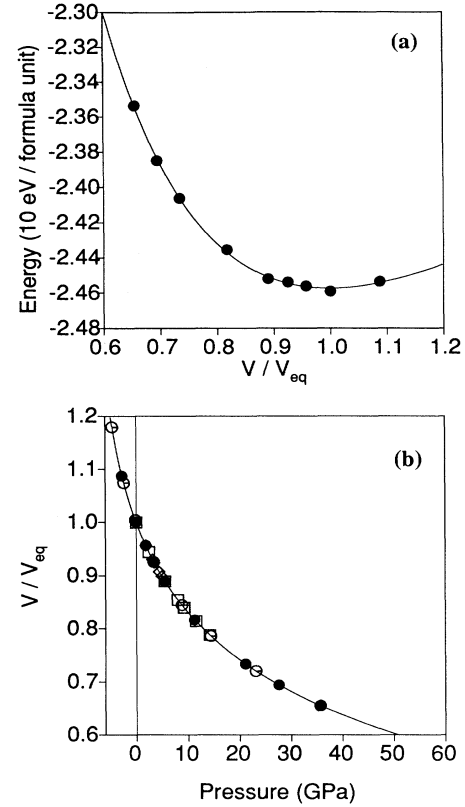


FIG. 2. (a) Calculated cohesive energy per formula unit versus volume. The volume values are normalized to the experimental volume at ambient pressure V_{eq} . The solid curve is a Birch-Murnaghan fit to the calculated points. (b) Equation of state for α -quartz. The volume is normalized to the experimental volume at ambient pressure. The solid curve represents the theoretical Birch-Murnaghan equation of state. (\bullet) represents our theoretical results, (\circ) results from Ref. 10, and (\square) and (\diamond) experimental data from Ref. 12 and Ref. 16, respectively.

TABLE II. Theoretical and experimental Birch-Murnaghan equation parameters for α -quartz. The volumes and the energies are expressed per formula unit. B_0 and B'_0 are the bulk modulus and its derivative with respect to pressure, respectively; V_0 indicates the equilibrium volume and E_0 the cohesive energy.

	B_0 (GPa)	B'_0	V_0 (\AA^3)	E_0 (eV)
Theory				
Present work	38.36	3.79	37.64	24.57
Chelikowsky <i>et al.</i> (Ref. 10) ^a	38.1	3.9	35.8	22.2
Experiment				
<i>CRC Handbook of Chemistry and Physics</i> (Ref. 26)				19.2
Levien <i>et al.</i> (Ref. 16)	38.±3.	6.0±0.2	37.71±0.01	
Hazen <i>et al.</i> (Ref. 12)	34.±3.	5.7±0.9	37.69±0.01	
Jorgensen (Ref. 21)	36.4±0.5	6.3±0.4	37.60±0.01	
D'Amour <i>et al.</i> (Ref. 22)	36.5±0.9	5.9±0.4	37.73±0.03	
Olinger and Halleck (Ref. 25)	38.±1.	5.4±0.4	37.67±0.01	
Vayda <i>et al.</i> (Ref. 25)	34.7±0.1	7.7±0.1	37.6	
McWhan (Ref. 25)	44.5±0.2	3.6±0.1		
McSkimin <i>et al.</i> (Ref. 25)	37.1±0.2	6.3±0.3		

^aMurnaghan equation parameters.

B. Structural properties under pressure

1. Lattice parameters and atomic fractional coordinates

We have also examined the deformation of α -quartz under pressure by studying the behavior of structural parameters, bond angles, and bond lengths with pressure in the range -3 to 36 GPa. In fact, unlike experiment, theory can determine structural variations for negative pressures, i.e., for expanded crystals.

We should remark that the determination of the B'_0 coefficient, being related to the third derivative of the E versus P function, is not straightforward and can be less accurate. In fact, from Table II it is possible to observe that our theoretical value, still being within the range of all the experiments considered, differs quite sensibly from the result by Levien *et al.*¹⁶ For this reason and in order to establish a common pressure scale with experimental works, we used the equation of state parameters from Levien *et al.*¹⁶ that, in our opinion, is the most recent and accurate work to date. Within this assumption, the pressure values explored by our calculations range from about -3 to 56 GPa.

In Table III we report the optimized structural parameters for the nine volumes analyzed. In Fig. 3 we plot the fractional coordinates variations with pressure. The $x(O)$ trend with pressure is mainly linear, while the other internal parameters tend to a saturation value. Our results agree well with experiment¹⁶ and previous theoretical work.¹⁰

It has been suggested^{12,15} that near the transition the oxygen atoms tend towards a body-centered-cubic array. The structural parameters derived considering an ideal bcc packing are $x(O) = y(O) = 1/3 \approx 0.3333$, $z(O) = 1/12 \approx 0.0833$, and $c/a = \sqrt{3}/2 \approx 1.2247$. In addition, assuming ideally centered SiO_4 tetrahedra, we obtain $x(\text{Si}) = 5/12 \approx 0.4167$. The results of our calculation seem to agree with this model. For the maximum compression considered, $V/V_{\text{eq}}=0.655$ (where V_{eq} represents the experimental volume at ambient pressure), the fractional coordinates obtained from first-principles calculations are, in fact, $x(O)=0.3480$, $y(O)=0.3320$, $z(O)=0.0795$, and $x(\text{Si})=0.4220$.

In Fig. 4 we show the projections along the c axis at room pressure (a) and at maximum compression $V/V_{\text{eq}}=0.655$ (b). Upon compression [Fig. 4(b)], it is

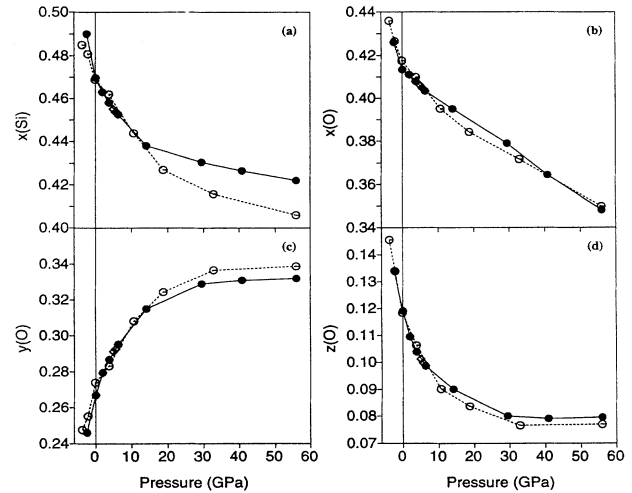


FIG. 3. Atomic fractional coordinates versus pressure and comparison with other theoretical works (Ref. 10) and experiment (Ref. 16). In (a) the silicon coordinate x is shown; in (b), (c), and (d) the oxygen coordinates x , y , and z are represented, respectively. (\bullet) indicates our theoretical results, (\circ) results from Ref. 10 and (\diamond) experimental data from Ref. 16.

easy to observe the reduction of the large open channels that α -quartz presents at ambient pressure. Moreover, the O atoms, joined by the dashed line [in (b)], form an hexagon, as expected for a bcc arrangement seen along the $[111]$ direction. This is in excellent agreement with Sowa's model¹⁵ and it is quantitatively confirmed by the values of the atomic fractional coordinates and the axial ratio c/a (as discussed below) obtained from our calculations. Of course this different arrangement of the oxygen atoms and the consequent more efficient packing will affect dramatically the electronic states involved in the bonds. We are not going to discuss this topic at length since this is beyond the aim of the present paper. The complete and thorough study of how the electronic states are affected by pressure application will be the subject of a forthcoming paper.²⁷

In Fig. 5 we report the c/a ratio as a function of pressure compared with theory¹⁰ and experiment.^{12,16} The agreement with experiment is excellent, while there are some discrepancies with the results by Chelikowsky *et al.*¹⁰ In fact, they pointed out that they found some dif-

TABLE III. Optimized structural parameters of α -quartz at a given unit cell volume. The parameters are determined minimizing the total energy of the system. V_{eq} represents the experimental volume at ambient pressure.

Volume (\AA^3)	V/V_{eq}	a (\AA)	c (\AA)	$x(\text{Si})$	$x(\text{O})$	$y(\text{O})$	$z(\text{O})$
123.001	1.087	5.0837	5.4955	0.4900	0.4260	0.2460	0.1340
113.131	1.000	4.9160	5.4054	0.4697	0.4135	0.2669	0.1191
108.242	0.957	4.8362	5.3439	0.4630	0.4111	0.2795	0.1095
104.612	0.925	4.7736	5.3010	0.4581	0.4079	0.2867	0.1039
100.646	0.890	4.7022	5.2561	0.4526	0.4034	0.2952	0.0987
92.412	0.817	4.5404	5.1761	0.4380	0.3950	0.3150	0.0900
83.000	0.734	4.3368	5.0957	0.4305	0.3790	0.3290	0.0800
78.540	0.694	4.2433	5.0368	0.4265	0.3645	0.3310	0.0790
74.091	0.655	4.1465	4.9758	0.4220	0.3480	0.3320	0.0795

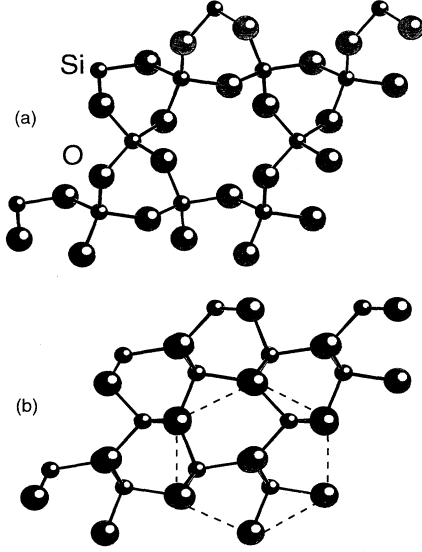


FIG. 4. Projections of the α -quartz structure along the c axis as optimized at room pressure (a), and at maximum compression $V/V_{\text{eq}} = 0.655$ (b). The oxygen atoms joined by the dashed line [in (b)] form a hexagon, as obtained by a bcc arrangement seen along the $[111]$ direction.

difficulties in reproducing the experimental changes of the c/a ratio.

At the maximum compression analyzed ($V/V_{\text{eq}} = 0.655$), c/a assumes the value 1.200, which is somewhat smaller than the expected ideal value for a perfect bcc packing of oxygen, yet still in good agreement with this model.

2. Axial and tetrahedral compressibilities

We would like to point out that the axial ratio is an important parameter which describes the anisotropic compression of α -quartz: The fact that c/a increases with pressure provides evidence of the different stiffness of the

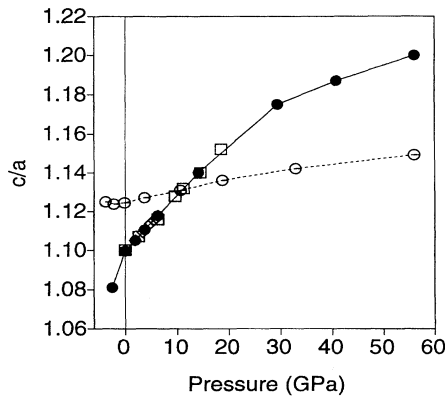


FIG. 5. c/a ratio versus pressure and comparison with other theoretical works (Ref. 10) and experiments (Refs. 12 and 16). Symbols are as in Fig. 2(b).

a and c axes. By using the formalism of elasticity theory, it is possible to make the connection between the variation of the c/a ratio and the crystal strain. In fact, the variation of the axial ratio can be expressed as a function of the finite Lagrangian tensor $\vec{\eta}$.²⁸ In this way, the increase of the axial ratio with pressure is found to be related to the different strain components along the directions parallel and perpendicular to the c axis, respectively.

The reduction of the lattice parameters as a function of pressure can be fitted by a second-order polynomial equation

$$\frac{a}{a_0} = 1 - \kappa_{a,0}P - \frac{1}{2} \left(\frac{\partial \kappa_a}{\partial P} \right)_0 P^2, \quad (1)$$

$$\frac{c}{c_0} = 1 - \kappa_{c,0}P - \frac{1}{2} \left(\frac{\partial \kappa_c}{\partial P} \right)_0 P^2, \quad (2)$$

where a_0 and c_0 are the zero-pressure lattice parameters, and $\kappa_{a,0} = -\frac{1}{a_0} \left(\frac{\partial a}{\partial P} \right)_0$ and $\kappa_{c,0} = -\frac{1}{c_0} \left(\frac{\partial c}{\partial P} \right)_0$ are the axial compressibilities. The values of the calculated coefficients obtained from the fit are $a_0 = 4.9232 \text{ \AA}$, $\kappa_{a,0} = 8.07 \times 10^{-3} \text{ GPa}^{-1}$, $\left(\frac{\partial \kappa_a}{\partial P} \right)_0 = -0.21 \times 10^{-3} \text{ GPa}^{-2}$, $c_0 = 5.3960 \text{ \AA}$, $\kappa_{c,0} = 4.13 \times 10^{-3} \text{ GPa}^{-1}$, and $\left(\frac{\partial \kappa_c}{\partial P} \right)_0 = -0.12 \times 10^{-3} \text{ GPa}^{-2}$. This implies that the c axis is approximately 2 times stiffer than the in-plane axes at zero pressure.

As a result, the spirals of the SiO_4 units (see Fig. 1) behave like stiff coiled springs along the c axis, and the deformation causes mainly the reduction of the large empty channels of α -quartz. This is quantitatively confirmed by the different variation of the volumes of the tetrahedron and of the cell with pressure, as shown in Fig. 6 (the values of the volume are expressed in units of the corresponding equilibrium quantities). We can observe a very small decrease of the volume of the tetrahedron upon compression; in fact, while the variation of the cell volume on the overall pressure range is about 34.5%, it is only 5.5% for the tetrahedron volume. By fitting the curve representing the tetrahedron volume as a function of pressure with a parabolic function [following Eqs. (1)

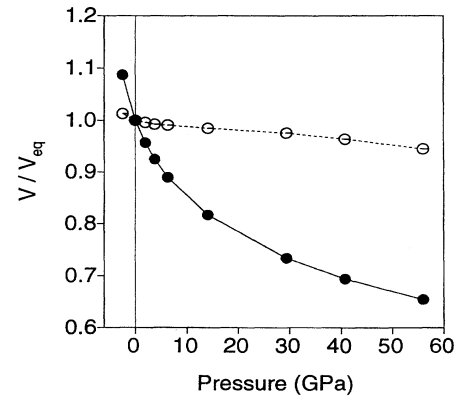


FIG. 6. Volume of the SiO_2 cell (\bullet) and of the SiO_4 tetrahedral unit (\circ) versus pressure. The values of the volumes are normalized to the corresponding equilibrium values.

and (2)], we obtain the corresponding compressibility. Its value is $0.14 \times 10^{-2} \text{ GPa}^{-1}$, which is about 20 times smaller than the compressibility of the overall crystal.

3. Deformation effects

While the overall volume of each tetrahedral unit is not drastically affected by pressure application, we find that pressure produces distortions of this unit. Let us look, for example, at the O-Si-O angles. They show little deviation from the ideal value 109.5° for pressures up to 6 GPa. Above this pressure, their deviation increases: The value for the smallest and largest angles at maximum compression are about 102° and 123° , respectively. In Fig. 7(a) theoretical O-Si-O angles are plotted and compared with experiment.¹⁶ We observe that three independent angles O-Si-O tend to the same value at highest pressures, in agreement with what found by Sowa.¹⁵

The mean bond length Si-O is substantially conserved, with a monotonic and slight decrease [see Fig. 7(b)]. At ambient pressure the mean distance Si-O is $\sim 1.61 \text{ \AA}$

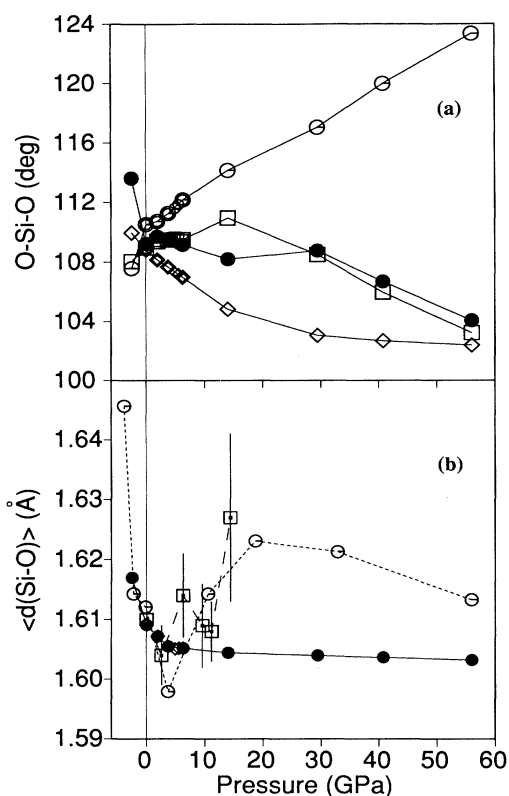


FIG. 7. (a) Theoretical O-Si-O bond angles versus pressure (large symbols) and comparison with experiment (Ref. 16) (small symbols). (\circ) and (\diamond) represent O-Si-O angles with twofold multiplicity; (\square) and (\bullet) correspond to O-Si-O angles with onefold multiplicity. The bond angles are indicated in Fig. 1. (b) Mean Si-O bond length versus pressure and comparison with other theoretical works (Ref. 10) and experiments (Refs. 12 and 16). Symbols are as in Fig. 2 (b). Vertical lines indicate the estimated standard deviations from Ref. 12.

and at $\sim 56 \text{ GPa}$ its value is $\sim 1.60 \text{ \AA}$. Our results are in good agreement with measurements by Levien *et al.*¹⁶ On the other hand, a previous theoretical work¹⁰ seems to find that the Si-O distance oscillates in the same range of pressure. This same result has been found also by Hazen *et al.*;¹² however, we have to point out that the measurements at high pressures are affected by large estimated standard deviations, as indicated in Fig. 7(b) by the vertical lines (e.g., at 12.5 GPa it is of the same order as the variation of the mean Si-O distance in the overall range of pressure).

In order to explain these findings, the possible change of Si coordination (from fourfold to sixfold or mixed fourfold and sixfold), induced by the formation of oxygen cubic packing,¹⁰ is often invoked. According to this model, the change in coordination would also imply an increase in the mean value of the Si-O distance. However, we should notice that, while this process may explain the diffraction data, it is not suitable to explain a theoretical calculation based on a fixed and well-defined geometry. In fact, a similar configuration could be obtained with a network of distorted tetrahedra, with silicon still chemically bonded to four oxygen atoms, although two other oxygen can be nearby²⁹ (at a distance larger than the bond length). This, of course, results in an increased average bond length, as measured by Hazen *et al.*¹² However, in the theoretical calculations, Si remains strictly tetrahedrally coordinated during the compression, since the spatial group of α -quartz is preserved. As a consequence, the regular and small decrease of the Si-O bond length upon compression is a correct and consistent finding.

In Figs. 8(a) and 8(b) we plot the variation of the intertetrahedral Si-O-Si angle and of the minimum O-O distance with pressure. Our trends are in good agreement with previous results.^{10,12,16} The dramatic decrease of the Si-O-Si angle and of the O-O distance reflects the reduction of structural voids. Hazen *et al.*¹² have tried to correlate the strains in the Si-O-Si angle with the transition to the amorphous phase. In particular, they suggested that the transition is driven by this small angle, which at 12.5 GPa is only 124° , less than any previously recorded average value.^{30,31} According to their theory, the transition should occur at about 15 GPa, since the extrapolated angle at this pressure is approximately 120° . In fact, from molecular orbital calculations³² of the strain energy as a function of the Si-O-Si angle it has been found that the strain energy increases abruptly as this angle goes below this value. Our theoretical results confirm approximately the boundary of the instability region (the Si-O-Si angle falls below 120° at pressures above $\sim 30 \text{ GPa}$), even if it is not in perfect agreement with some of the experimental findings.

Let us look now at how the connection between different tetrahedral units is affected by pressure. The interpolyhedral O-O compression is directly related to the bending of the Si-O-Si angle. The decrease of the O-O distance represents, therefore, a measure of the reduction of structural voids: As discussed before, the volume of the tetrahedra SiO_4 is substantially conserved and the compressibility of the crystal structure is much larger

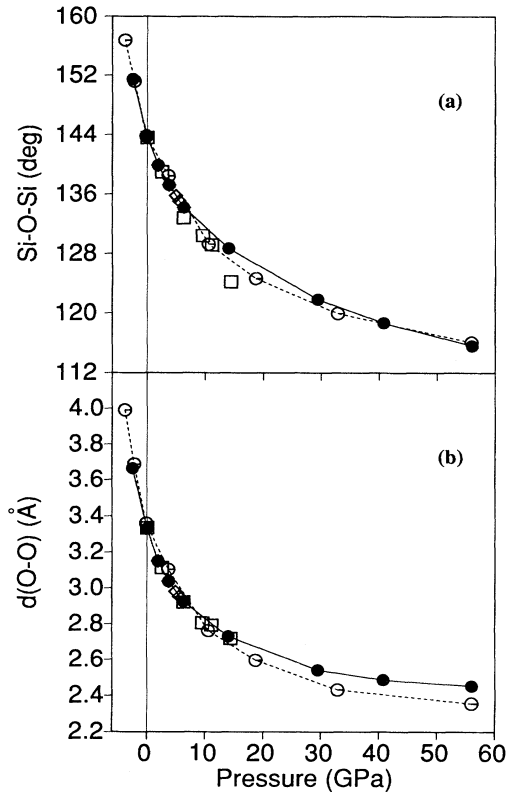


FIG. 8. Intertetrahedral Si-O-Si angle (a) and minimum O-O distance (b) versus pressure and comparison with other theoretical works (Ref. 10) and experiments (Refs. 12 and 16). Symbols are as in Fig. 2(b). The bond angle and the O-O distance are those indicated in Fig. 1.

than that of a single tetrahedral unit. Among the various O-O distances that can be defined in the structure, the minimum one changes from 3.33 Å at ambient pressure to 2.73 Å at ~14 GPa; this value is very close to the shortest known interpolyhedral distance in ordered silicates [i.e., 2.75 Å occurring in Be_2SiO_4 Ref. (33)].

4. Structural properties and the transition to the amorphous state

A possible criterion to establish the occurrence of the transition is to consider the minimal values (of angles and/or bonds) observed in the wide variety of ordered silicates. This criterion has been established by experimentalists from the observation of diffraction data on samples close to the transition, and it is quite widely recognized. Therefore, using this same criterion, we can individuate a possible range of order instability looking at our theoretical trends for the Si-O-Si angle and the O-O distance as a function of pressure. The decrease of these structural parameters below the smallest value experimentally observed indicates pressures between 15 and 30 GPa as a possible range for an order-disorder transition. The rapid variation of these related parameters measures the enormous decrease of the structural voids; the large increase of the strain energy associated

with this deformation could be therefore the cause of the transition to the amorphous state. In fact, if we look at the possible onset of the amorphization (15–30 GPa) we find, correspondingly, a large decrease of the calculated cohesive energy (from 0.24 to 0.54 eV per formula unit with respect to the equilibrium structure). However, we should keep in mind that this is only a semiquantitative indication of the limit conditions reached by α -quartz and its incipient amorphization.

On the other hand, we should point out that it is very difficult to determine the exact value of the transition pressure also experimentally. This is the reason why the quartz amorphization is still an open issue.

Many models have been suggested in order to explain the amorphization mechanism in α -quartz. Among the others, Sowa¹⁵ proposed that the amorphization may happen through a structural transformation into a bcc-like arrangement of oxygen atoms. This structure is the same we find at very high pressure (56 GPa) (discussed before, in Sec. III B 1). We can notice that the bcc lattice has both octahedral and tetrahedral sites, but only one of the tetrahedral sites is occupied by a silicon. This is already a possible cause of disorder; moreover, if the energy needed by Si to diffuse towards neighboring octahedral sites or between tetrahedral sites is small, then this process can be a possible mechanism to produce a disordered phase. Of course, this is only one of the possible processes that might determine quartz amorphization and it is only partially supported by theoretical calculations since the bcc arrangement is found to exist (in our calculations) only at high pressures.

IV. CONCLUSIONS

We have presented all-electron calculations, based on the FLAPW method, on the structural behavior and the elastic properties of α -quartz under high-pressure. We examined the structural deformation near and above the amorphous transition, preserving the crystalline symmetry, with no loss of accuracy at high-pressure values.

Upon compression, we observed a slight distortion of the SiO_4 units, which substantially conserve their volume. We find that the average Si-O bond length presents a monotonic and very small decrease; at higher pressure it tends to a saturation value, which is very close to the value at the equilibrium. The trend of the c/a ratio is in good agreement with experiment; at the maximum compression considered, its value matches very closely the corresponding value of Sowa's model.

Our results suggest that the order-disorder transition is driven by the intertetrahedral O-O distance and the Si-O-Si angle. These are related parameters rapidly varying with pressure: They decrease below the smallest values occurring on crystalline silicates, causing an enormous reduction of structural voids.

ACKNOWLEDGMENT

This work was supported by Grant No. 92/1222-5 at Cineca (Casalecchio di Reno-Bologna-Italy).

- ¹ H. D. Megaw, *Crystal Structure: A Working Approach* (Saunders, Philadelphia, 1973); R. Calas, P. Pascal, and J. Wyart, *Nouveau Traité de Chimie Minérale* (Masson et Cie Éd., Paris, 1965).
- ² A. C. Lasaga and G. V. Gibbs, *Phys. Chem. Miner.* **14**, 107 (1987).
- ³ S. Tsuneyuki, M. Tsukada, H. Aoki, and Y. Matsui, *Phys. Rev. Lett.* **61**, 869 (1988).
- ⁴ S. Tsuneyuki, Y. Matsui, H. Aoki, and M. Tsukada, *Nature* **339**, 209 (1989).
- ⁵ S. Tsuneyuki, H. Aoki, M. Tsukada, and Y. Matsui, *Phys. Rev. Lett.* **64**, 776 (1990); J. R. Chelikowsky, H. E. King, Jr., and J. Glinnemann, *Phys. Rev. B* **41**, 10866 (1990); J. S. Tse and D. D. Klug, *Phys. Rev. Lett.* **67**, 3559 (1991).
- ⁶ L. V. Woodcock, C. A. Angell, and P. Cheeseman, *J. Chem. Phys.* **65**, 1565 (1976).
- ⁷ R. Dovesi, C. Pisani, and C. Roetti, *J. Chem. Phys.* **86**, 6967 (1987); B. Silvi, P. D'Arco, and M. Causà, *ibid.* **93**, 7225 (1990); R. Nada, C. R. A. Catlow, R. Dovesi, and C. Pisani, *Phys. Chem. Miner.* **17**, 353 (1990).
- ⁸ D. C. Allan and M. P. Teter, *Phys. Rev. Lett.* **59**, 1136 (1987).
- ⁹ K. T. Park, K. Terakura, and Y. Matsui, *Nature* **336**, 670 (1988).
- ¹⁰ J. R. Chelikowsky, H. E. King, Jr., N. Troullier, J. L. Martins, and J. Glinnemann, *Phys. Rev. Lett.* **65**, 3309 (1990); J. R. Chelikowsky, N. Troullier, J. L. Martins, and H. E. King, Jr., *Phys. Rev. B* **44**, 489 (1991); N. Binggeli, N. Troullier, J. L. Martins and J. R. Chelikowsky, *ibid.* **44**, 4471 (1991); N. Binggeli and J. R. Chelikowsky, *Nature* **353**, 344 (1991); *Phys. Rev. Lett.* **69**, 2220 (1992).
- ¹¹ R. J. Hemley, A. P. Jephcoat, H. K. Mao, L. C. Ming, and M. H. Manghnani, *Nature* **334**, 52 (1988).
- ¹² R. M. Hazen, L. W. Finger, R. J. Hemley, and H. K. Mao, *Solid State Commun.* **72**, 507 (1989).
- ¹³ O. Mishima, L. D. Calvert, and E. Whalley, *Nature* **310**, 393 (1984); G. C. Serghiou, R. R. Winters, and W. S. Hammack, *Phys. Rev. Lett.* **68**, 3311 (1992).
- ¹⁴ M. B. Kruger and R. Jeanloz, *Science* **249**, 647 (1990).
- ¹⁵ H. Sowa, *Z. Kristallogr.* **184**, 257 (1988).
- ¹⁶ L. Levien, C. T. Prewitt, and D. J. Weidner, *Am. Mineral.* **65**, 920 (1980).
- ¹⁷ L. Hedin and B. I. Lundqvist, *J. Phys. C* **4**, 2064 (1971).
- ¹⁸ H. J. F. Jansen and A. J. Freeman, *Phys. Rev. B* **30**, 561 (1984).
- ¹⁹ D. J. Chadi and H. L. Cohen, *Phys. Rev. B* **8**, 5747 (1973); H. J. Monkhorst and J. P. Pack, *ibid.* **13**, 5188 (1976).
- ²⁰ G. S. Smith and L. E. Alexander, *Acta Crystallogr.* **16**, 462 (1963); Y. Le Page and G. Donnay, *Acta Crystallogr. B* **32**, 2456 (1976).
- ²¹ J. D. Jorgensen, *J. Appl. Phys.* **49**, 5473 (1978).
- ²² H. D'Amour, W. Denner, and H. Schulz, *Acta Crystallogr. B* **35**, 550 (1979).
- ²³ *International Tables for X-ray Crystallography* (Kynoch Press, Birmingham, 1974).
- ²⁴ K. Y. Kim and A. L. Ruoff, *J. Appl. Phys.* **52**, 245 (1981).
- ²⁵ H. J. McSkimin, P. Andreatch, Jr., and R. N. Thurston, *J. Appl. Phys.* **36**, 1624 (1965); D. B. McWhan, *ibid.* **38**, 347 (1967); S. N. Vayda, S. Bailey, T. Pasternak, and G. C. Kennedy, *J. Geophys. Res.* **78**, 6893 (1973); B. Olinger and P. M. Halleck, *ibid.* **81**, 5711 (1976).
- ²⁶ *CRC Handbook of Chemistry and Physics*, 64th ed. (CRC, Boca Raton, FL, 1983).
- ²⁷ A. Di Pomponio and A. Continenza (unpublished).
- ²⁸ M. Catti, *Acta Crystallogr. A* **41**, 494 (1985); D. C. Wallace, *Thermodynamics of Crystals* (Wiley, New York, 1972); J. F. Nye, *Propriétés Physiques des Cristaux* (Dunod Éd., Paris, 1961).
- ²⁹ E. M. Stolper and T. J. Ahrens, *Geophys. Res. Lett.* **14**, 1231 (1987).
- ³⁰ F. Liebau, *Structural Chemistry of Silicates* (Springer, New York, 1985).
- ³¹ J. A. Tossel and G. V. Gibbs, *Acta Crystallogr. A* **34**, 463 (1978).
- ³² K. L. Geisinger, G. V. Gibbs, and A. Navrotsky, *Phys. Chem. Miner.* **11**, 266 (1985).
- ³³ J. Zemann, *Z. Kristallogr.* **175**, 299 (1986).